
REPORT No. 217

PRELIMINARY WING MODEL TESTS IN THE VARIABLE DENSITY WIND TUNNEL OF THE NATIONAL ADVISORY COMMITTEE FOR AERONAUTICS

By MAX M. MUNK
National Advisory Committee
for Aeronautics

REPORT No. 217

PRELIMINARY WING MODEL TESTS IN THE VARIABLE DENSITY WIND TUNNEL OF THE NATIONAL ADVISORY COMMITTEE FOR AERONAUTICS

By MAX M. MUNK

S U M M A R Y

The following report contains the results of a series of tests with three wing models. By changing the section of one of the models and painting the surface of another, the number of models tested was increased to five. The tests were made in order to obtain some general information on the air forces on wing sections at a high Reynolds Number and in particular to make sure that the Reynolds Number is really the important factor, and not other things like the roughness of the surface and the sharpness of the trailing edge.

The few tests described below seem to indicate that the air forces at a high Reynolds Number are not equivalent to respective air forces at a low Reynolds Number (as in an ordinary atmospheric wind tunnel). The drag appears smaller at a high Reynolds Number and the maximum lift is increased in some cases. The roughness of the surface and the sharpness of the trailing edge do not materially change the results, so that we feel confident that tests with systematic series of different wing sections will bring consistent results, important and highly useful for the designer.

ARRANGEMENT OF TESTS

The models used in the tests described in this report were made of aluminum and were smoothly cut to shape, without any polishing.

The chord was 5 in., the span 30 in., which latter is half the throat diameter of the wind tunnel. This ratio is so large that the influence of the tunnel walls begins to be perceptible. The actual aspect ratio of the wing models, which were square and not warped, was 6; but the influence of the walls theoretically changes the air forces as if the aspect ratio had been 6.85.

This report contains all forces and angles of attack as actually observed, making no allowance for the influence of the tunnel walls. We have inserted in the diagrams the parabola of the induced drag for an aspect ratio of 6.85. (References 1 and 2.)

Figure 1 shows diagrammatically how the models were attached to the balance ring. It is a combination of wire attachment and rigid connection. A pair of vertical wires *A* are stretched from top to bottom of the balance ring. These wires are connected to the wing at one quarter of the chord behind the leading edge. Furthermore, one skid *B*, screwed to the wing, is hinged to a vertical bar *C*, which runs across the air stream and can be moved up and down. The bar is well shielded from the air stream by a tube in which it slides and its motion is used to change the angle of attack.

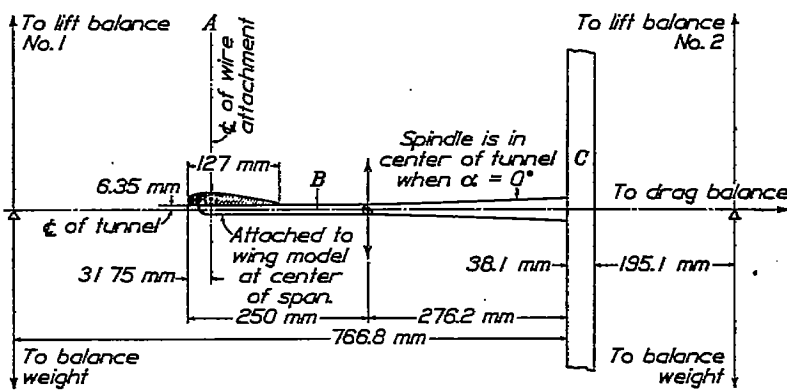
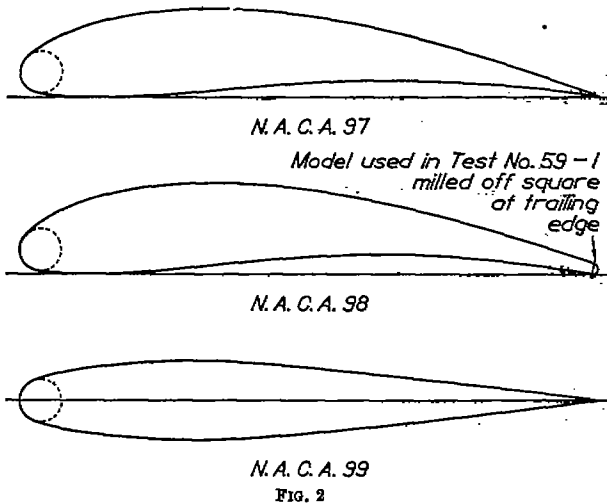


FIG. 1

RESULTS

The results are given in the figures and tables, both of which contain the conditions of each test. There is also a table of ordinates of the three wing sections Nos. 97, 98, and 99. Moreover, the cambered section 98 with round rear edge was milled off to obtain a square end, and the cambered section No. 97 (with a sharp trailing edge), Figure 2, was covered with oil paint after the test had been finished, to study the influence of the surface roughness.



The coefficient of the component of the air force at right angles to the chord is

$$C_R = C_L \cos \alpha + C_D \sin \alpha.$$

Hence the center of pressure can be computed from the moment coefficient, the lift coefficient and the drag coefficient by means of the formula

$$C.P. = 25\% - \frac{C_M}{C_L \cos \alpha + C_D \sin \alpha} \cdot 100\%.$$

C.P. denotes here the distance in per cent of the chord from the leading edge. The moment coefficient is derived from the moment itself by dividing it by the dynamical pressure $V^2 \frac{\rho}{2}$ and by the product of the wing area and the mean chord of the wing.

In the figures the lift coefficient $\frac{L}{S_q}$ is plotted upward. The induced drag coefficient for an aspect ratio of 6.85, the observed drag coefficient, and the moment coefficient $\frac{M}{cS_q}$ are plotted against the lift coefficient to the right. The value of the angle of attack is inserted along the lift-drag curve.

Figures 3 to 8 refer to the strut section. The moment is expected to be zero and is nearly so in the figures. The small difference can be explained by taking into account the effect of the finite curvature at the leading edge. The reader will observe that at high pressure the wing shows a marked improvement; the minimum and the mean drag coefficient decreases, while the lift coefficient increases from 0.79 to 1.1. Figures 9 to 14 are corresponding tests with a cambered section of the same thickness. Here we observe the same decrease of the drag coefficient when the Reynolds Number increases, but the maximum lift keeps about constant. It just happens to be slightly larger at 16 atmospheres but resumes its old value at 20.9 atmospheres. The moment curve in Figure 12 coincides with the theoretical vertical straight line quite closely. Figure 14 gives the results for the same model not painted. The increase of roughness was easily felt by touching the model. The difference in the result is, however, of no important magnitude.

We have, therefore, 5 different models, each of which could be measured at different density of the air. All in all, we have made 18 different runs, each time varying the angle of attack within a large range and determining the lift and drag. In some of the tests we have also determined the pitching moment with respect to a point on the chord and at one quarter of the chord behind the leading edge. The moment is considered positive if it makes the leading edge rise. This reference point is of special importance; the theory of thin wing section gives a pitching moment with respect to this point independent of the angle of attack. This makes it more convenient for practical use. (Reference 2.)

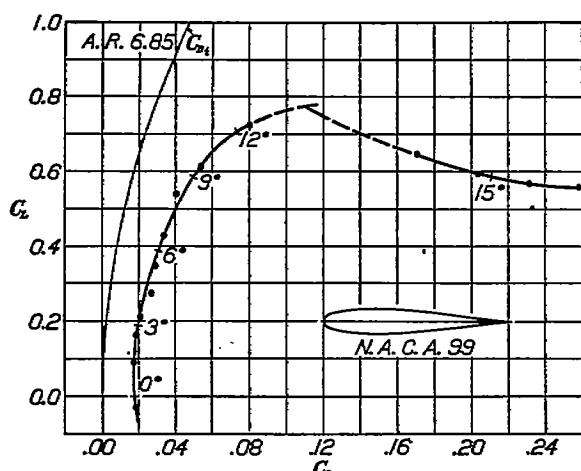


FIG. 3.—Test No. 56-1. Tank pressure 1 atmosphere. Dynamic pressure $q=27.5 \text{ kg/m}^2$. Reynolds Number 175,000

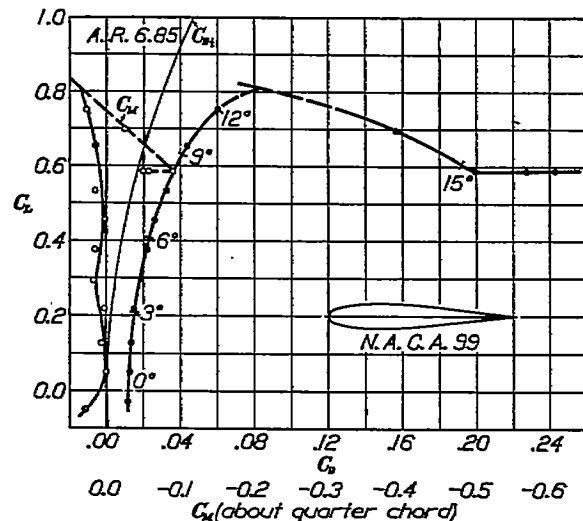


FIG. 4.—Test No. 56-3. Tank pressure 2.03 atmospheres. Dynamic pressure $q=57.3 \text{ kg/m}^2$. Reynolds Number 352,000

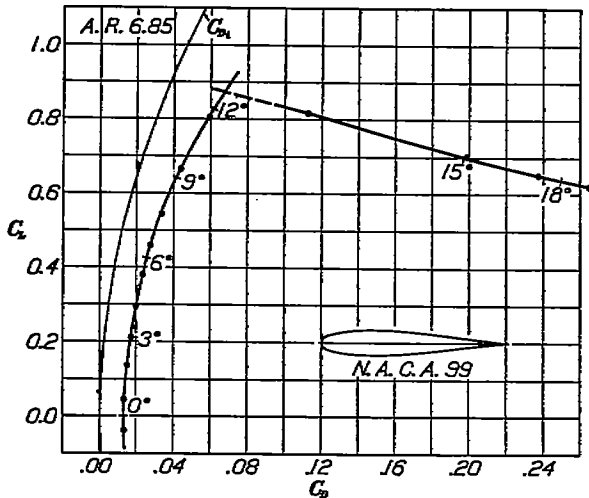


FIG. 5.—Test No. 56-5. Tank pressure 4.05 atmospheres. Dynamic pressure $q=120 \text{ kg/m}^2$. Reynolds Number 719,000

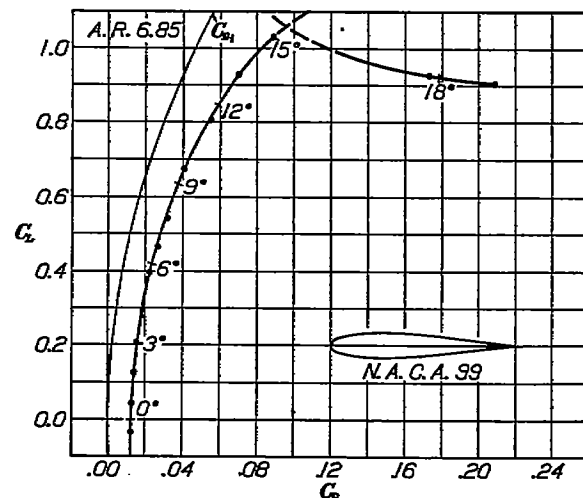


FIG. 6.—Test No. 56-7. Tank pressure 6.0 atmospheres. Dynamic pressure $q=183 \text{ kg/m}^2$. Reynolds Number 1,070,000

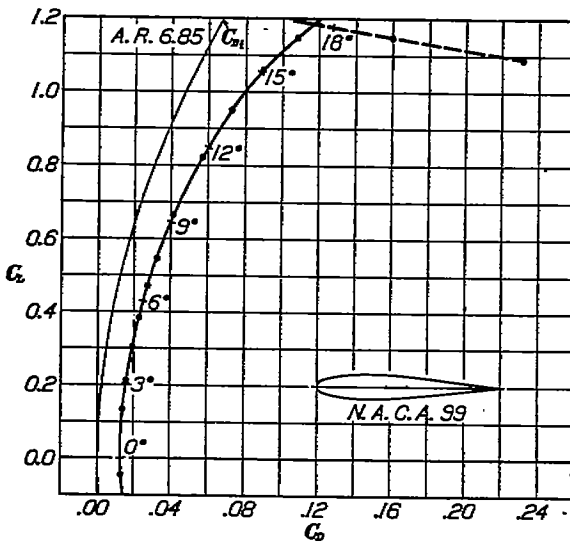


FIG. 7.—Test No. 56-9. Tank pressure 8.3 atmospheres. Dynamic pressure $q=256 \text{ kg/m}^2$. Reynolds Number 1,449,000

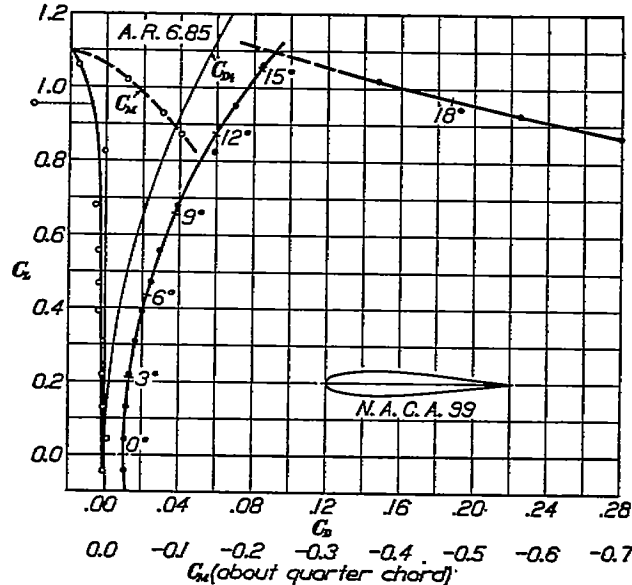


FIG. 8.—Test No. 56-11. Tank pressure 16.24 atmospheres. Dynamic pressure $q=543 \text{ kg/m}^2$. Reynolds Number 2,950,000

The remaining tests, Figures 15 to 19, were made on the cambered section with different trailing edges. The thick rounding of the rear edge of course increases the drag but does not otherwise change the character of the result. The same holds true for Figure 20 with the square trailing edge.

DISCUSSION OF RESULTS

The tests suggest the general rule that at a full Reynolds Number the cambered wing has a smaller drag, the symmetrical section both a smaller drag and a larger maximum lift than in the old type wind tunnel. The roughness of the surface and the sharpness of the trailing edge, if reasonably chosen, have no influence on the results. The results, as those in any wind tunnel should not be scrutinized too closely and not too literally interpreted. The new tunnel will show the direction and the way to the improvement of aircraft, but the results with a square wing alone in an airflow without fuselage and propeller can not give absolute information regarding the air forces on the wings of a real airplane. However, the results obtained give us the right to expect confidently consistent and qualitative results from the investigation of a systematic series of wing models now to be taken up, as likewise from later studies of wings with ailerons and of combinations of several parts of the airplane at full-size Reynolds Number.

TABLE I

SECTION NO. N. A. C. A. 97. FICTITIOUS ASPECT RATIO, MODEL NO. 9. 6.85. SPAN 30 IN., 76.2 cm. CHORD 5 IN., 12.7 cm. AREA, 0.0968 m². ASPECT RATIO, 6.

Angle of attack, degree	$\frac{q}{kg/m^2}$	Lift $\frac{L}{kg}$	Lift coef. C_L	Drag coef. C_D	Moment coef. C_M
-11.6	27.4	-0.18	-0.068	0.0353	-0.063
-9.2	27.5	-0.04	-0.015	0.0705	-0.106
-6.7	27.5	.50	.186	0.0242	-0.202
-4.1	27.5	.95	.357	0.0287	-0.156
-2.8	27.5	1.23	.402	0.0272	-0.197
-1.7	27.5	1.47	.551	0.0322	-0.179
-1.4	27.5	1.76	.661	0.0389	-0.180
-8	27.5	1.95	.778	0.0440	-0.200
2.1	27.5	2.18	.820	0.0529	-0.159
3.2	27.5	2.40	.904	0.0601	-0.127
5.6	27.5	2.81	1.05	0.0806	-0.133
7.9	27.5	3.21	1.21	0.0961	-0.117
10.5	27.5	3.51	1.32	0.1242	-0.050
13.4	27.5	3.62	1.38	0.1385	-0.048
14.7	27.5	3.63	1.37	0.1781	-0.024
15.9	27.5	3.60	1.38	0.1970	-0.037
17.0	27.5	3.58	1.38	0.2160	-0.006
18.4	27.5	3.55	1.34	0.2340	.024

TABLE III

SECTION NO. N. A. C. A. 97. FICTITIOUS ASPECT RATIO, MODEL NO. 9. 6.85. SPAN 30 IN., 76.2 cm. CHORD 5 IN., 12.7 cm. AREA, 0.0968 m². ASPECT RATIO, 6.

Angle of attack, degree	$\frac{q}{kg/m^2}$	Lift $\frac{L}{kg}$	Lift coef. C_L	Drag coef. C_D
-11.6	246	-5.03	-0.211	0.0182
-9.2	246	-3.80	-0.333	0.0187
-6.7	246	3.61	.151	0.0139
-4.1	246	7.59	.818	0.0173
-2.8	246	10.24	.429	0.0214
-1.7	246	12.40	.511	0.0264
-1.4	246	14.48	.608	0.0323
-8	246	16.77	.705	0.0395
2.1	246	18.50	.778	0.0463
5.2	246	20.58	.864	0.0548
5.8	246	24.39	1.03	0.0740
7.9	246	27.23	1.14	0.0956
10.5	246	29.98	1.26	0.1250
13.4	246	31.77	1.34	0.1553
14.7	246	32.21	1.36	0.1699
16.9	246	32.31	1.36	0.2023
17.0	246	32.83	1.36	0.2276
18.4	246	31.98	1.35	0.2514
19.8	244	31.64	1.35	0.2800
21.1	244	31.07	1.32	0.3000
22.3	243	30.62	1.31	0.3230

TABLE II

SECTION NO. N. A. C. A. 97. FICTITIOUS ASPECT RATIO, MODEL NO. 9. 6.85. SPAN 30 IN., 76.2 cm. CHORD 5 IN., 12.7 cm. AREA, 0.0968 m². ASPECT RATIO, 6. REYNOLDS NUMBER, 740,000.

Angle of attack, degree	$\frac{q}{kg/m^2}$	Lift $\frac{L}{kg}$	Lift coef. C_L	Drag coef. C_D
-11.6	122	-1.42	-0.119	0.0104
-9.2	122	-1.14	-.012	0.0141
-6.7	122	1.91	.101	0.0121
-4.2	122	4.15	.349	0.0154
-2.8	122	5.32	.445	0.0195
-1.6	122	6.47	.544	0.0257
-1.4	122	7.47	.627	0.0309
.8	122	8.59	.722	0.0378
2.1	122	9.56	.805	0.0460
3.2	122	10.61	.892	0.0535
5.6	122	12.53	1.08	0.0735
7.9	122	13.99	1.17	0.0933
10.6	122	15.10	1.27	0.1215
13.4	122	15.82	1.32	0.1607
14.7	122	15.77	1.33	0.1927
15.9	122	15.74	1.33	0.2027
17.0	122	15.67	1.33	0.2240
18.4	122	15.50	1.31	0.2480
19.8	122	15.29	1.29	0.2735
21.1	122	15.00	1.27	0.2933
22.3	120	14.77	1.27	0.3200

TABLE IV

SECTION NO. N. A. C. A. 97. FICTITIOUS ASPECT RATIO, MODEL NO. 9. 6.85. SPAN 30 IN., 76.2 cm. CHORD 5 IN., 12.7 cm. AREA, 0.0968 m². ASPECT RATIO, 6. REYNOLDS NUMBER, 2,810,000.

Angle of attack, degree	$\frac{q}{kg/m^2}$	Lift $\frac{L}{kg}$	Lift coef. C_L	Drag coef. C_D	Moment about $c/4$ $\frac{kg \cdot cm}{kg \cdot m}$	Moment coef. C_M
-11.6	524	-11.04	-0.230	0.0156	139.0	0.217
-9.2	522	-2.43	-.048	0.0106	-88.9	-1.138
-6.7	525	6.23	.123	0.0102	-90.9	-1.141
-4.2	525	16.39	.323	0.0150	-88.9	-1.138
-2.8	525	21.06	.416	0.0186	-86.6	-1.133
-1.6	523	24.37	.481	0.0212	-80.2	-0.032
-1.4	523	28.57	.565	0.0281	-58.8	-0.079
.8	523	33.65	.605	0.0339	-18.6	-0.029
2.1	523	33.71	.783	0.0416	-80.6	-0.126
3.2	524	43.20	.855	0.0525	-83.7	-0.130
5.6	524	51.96	1.023	0.0743	-87.8	-0.136
7.9	524	58.79	1.16	0.0966	-82.5	-0.128
10.6	528	65.38	1.28	0.1285	-68.8	-0.008
13.4	528	68.28	1.34	0.1428	-67.6	-0.104
14.7	530	70.65	1.38	0.1680	-69.5	-0.139
15.9	528	70.63	1.38	0.1908	-68.8	-0.120
17.0	527	69.92	1.37	0.2147	-84.7	-0.131
18.4	527	68.65	1.34	0.2339	-86.0	-0.133
19.8	524	67.25	1.33	0.2630	-82.6	-0.143
21.1	523	65.65	1.30	0.3109	-84.4	-0.150

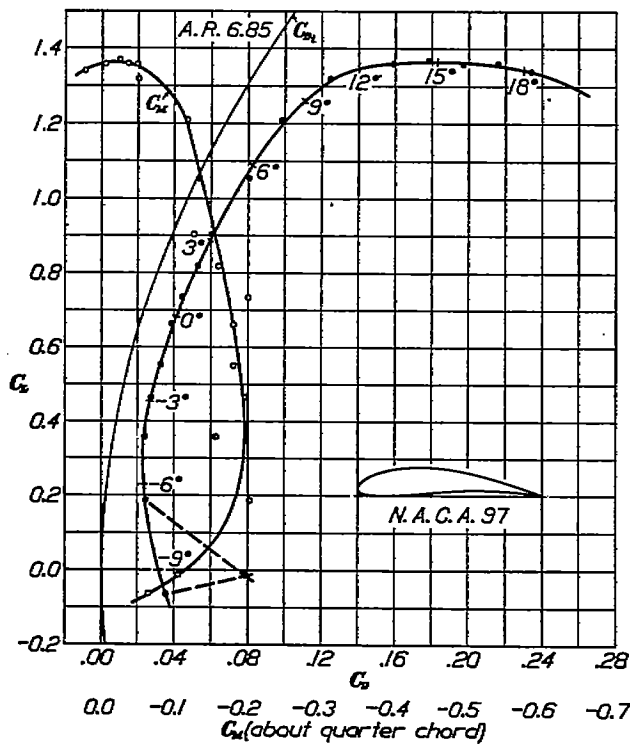


FIG. 9.—Test No. 58-1. Tank pressure 1.0 atmosphere. Dynamic pressure $q = 27.5 \text{ kg/m}^2$. Reynolds Number 175,000

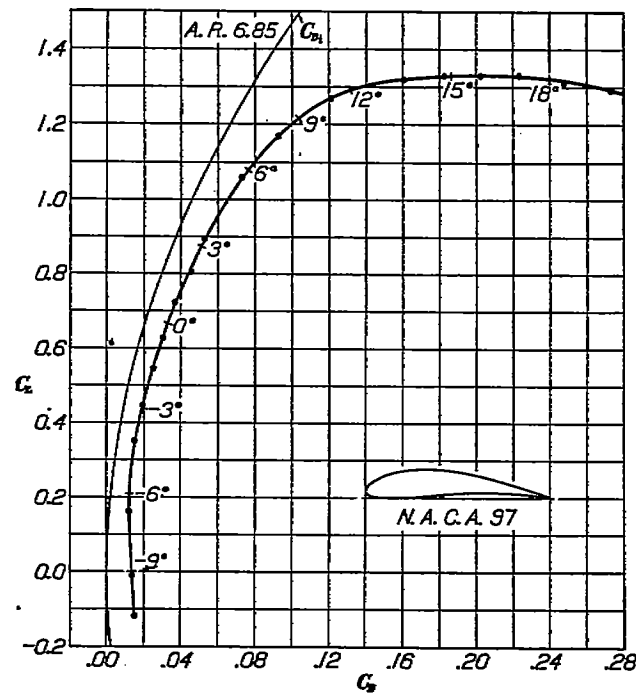


FIG. 10.—Test No. 58-2. Tank pressure 4.1 atmospheres. Dynamic pressure $q = 122 \text{ kg/m}^2$. Reynolds Number 740,000

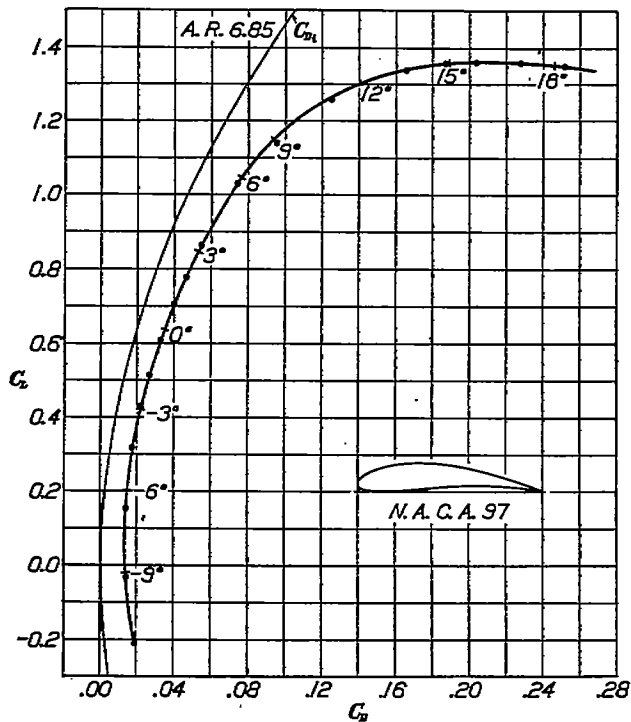


FIG. 11.—Test No. 58-3. Tank pressure 8 atmospheres. Dynamic pressure $q = 216 \text{ kg/m}^2$. Reynolds Number 1,430,000

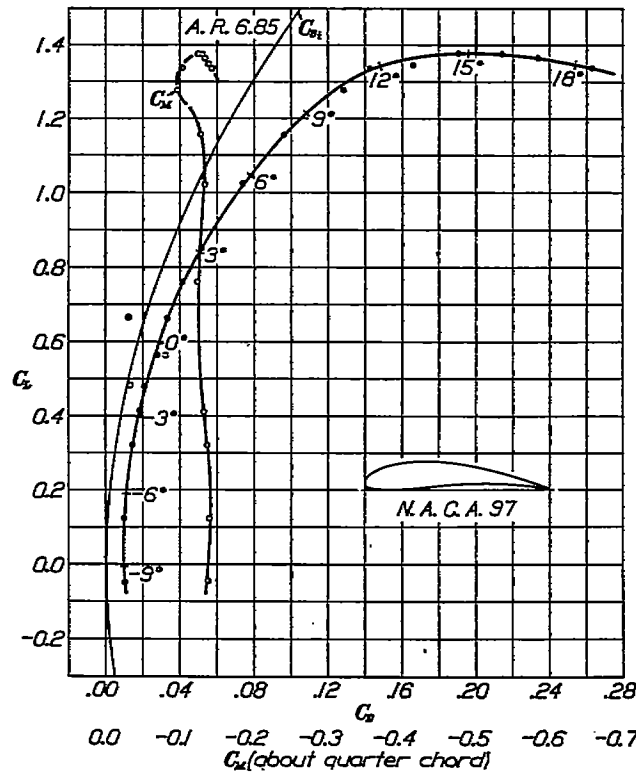


FIG. 12.—Test No. 58-4. Tank pressure 16 atmospheres. Dynamic pressure $q = 524 \text{ kg/m}^2$. Reynolds Number 2,810,000

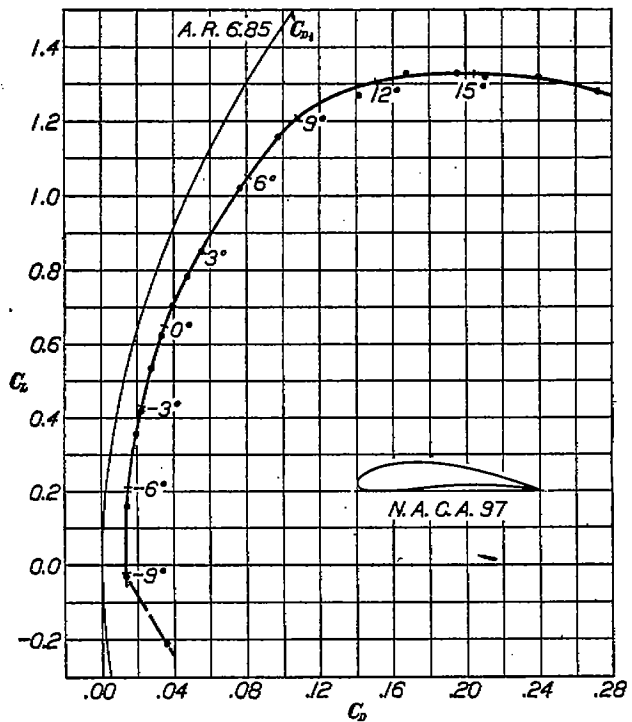


FIG. 13.—Test No. 58-5. Tank pressure 20.9 atmospheres. Dynamic pressure $q=705 \text{ kg/m}^2$. Reynolds Number 3,850,000

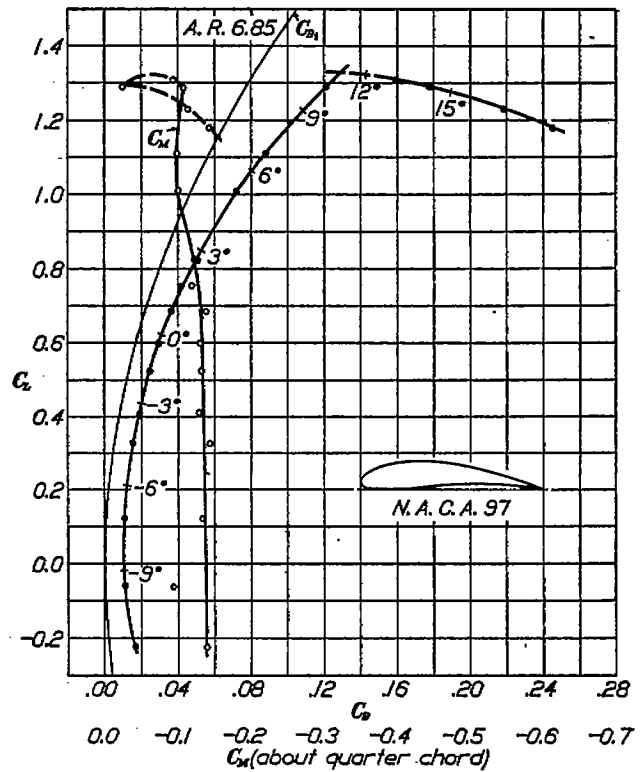


FIG. 14.—Test No. 61-3. Tank pressure 16.7 atmospheres. Dynamic pressure $q=587 \text{ kg/m}^2$. Reynolds Number 3,080,000. Airfoil painted

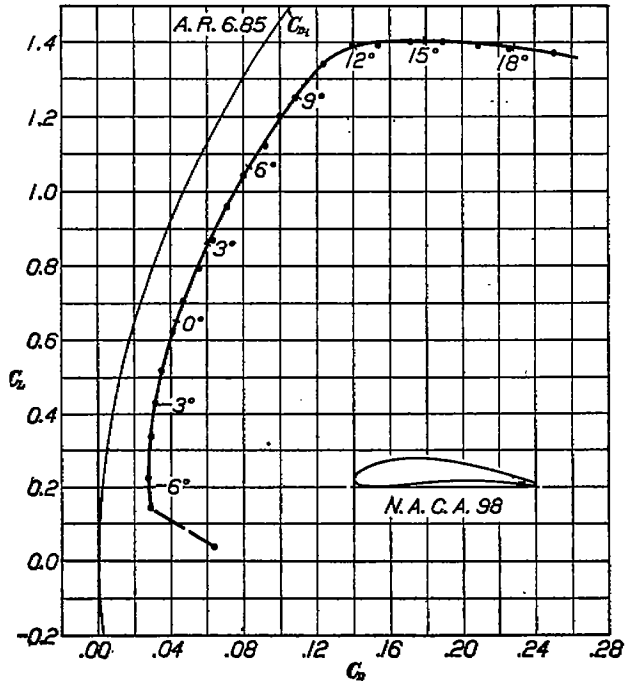


FIG. 15.—Test No. 57-1. Tank pressure 1.0 atmosphere. Dynamic pressure $q=27.8 \text{ kg/m}^2$. Reynolds Number 170,000

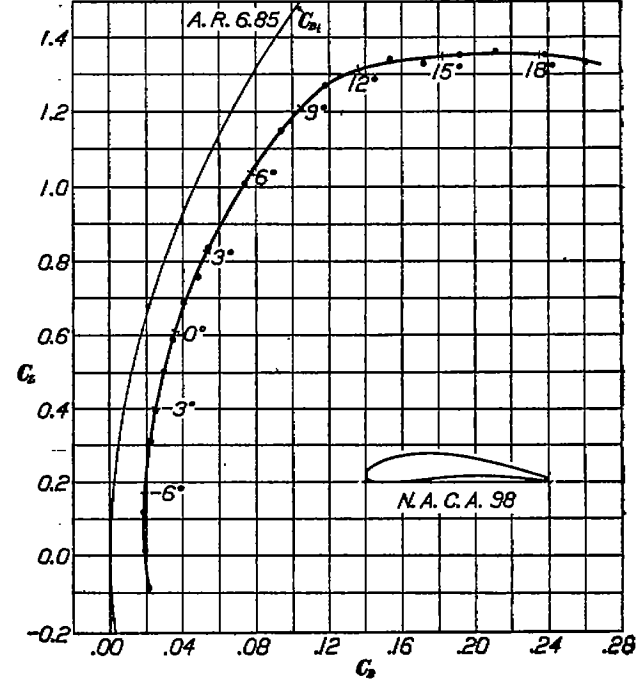


FIG. 16.—Test No. 57-2. Tank pressure 4.15 atmospheres. Dynamic pressure $q=123 \text{ kg/m}^2$. Reynolds Number 755,000

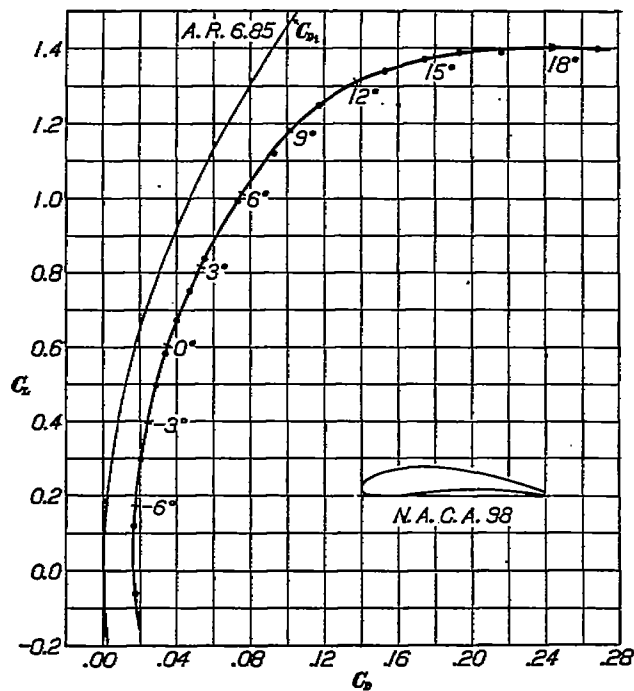


FIG. 17.—Test No. 57-3. Tank pressure 8.2 atmospheres. Dynamic pressure $q=258 \text{ kg/m}^2$. Reynolds Number 1,490,000

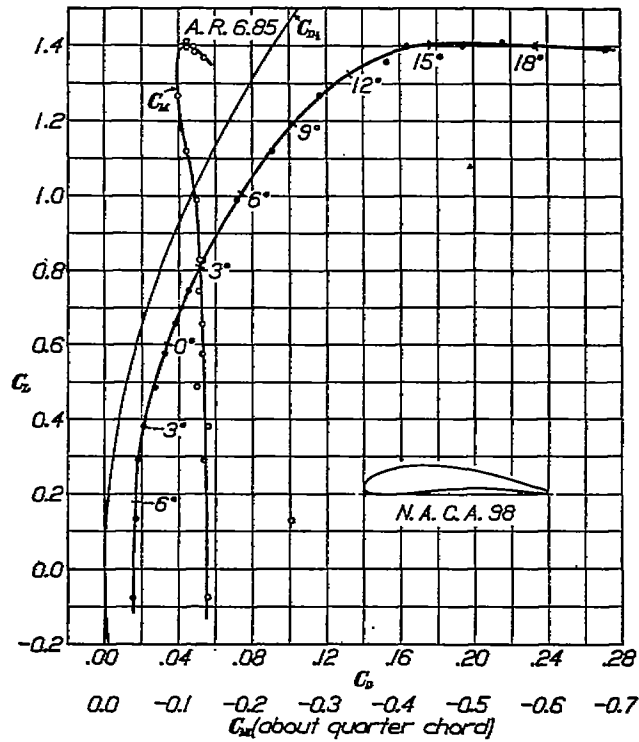


FIG. 18.—Test No. 57-4. Tank pressure 16.44 atmospheres. Dynamic pressure $q=531 \text{ kg/m}^2$. Reynolds Number 2,880,000

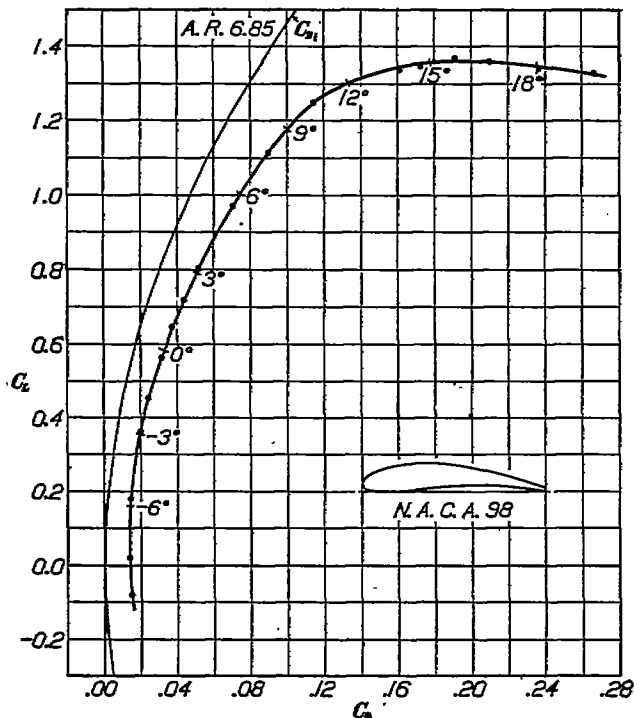


FIG. 19.—Test No. 57-5. Tank pressure 20.4 atmospheres. Dynamic pressure $q=699 \text{ kg/m}^2$. Reynolds Number 3,730,000

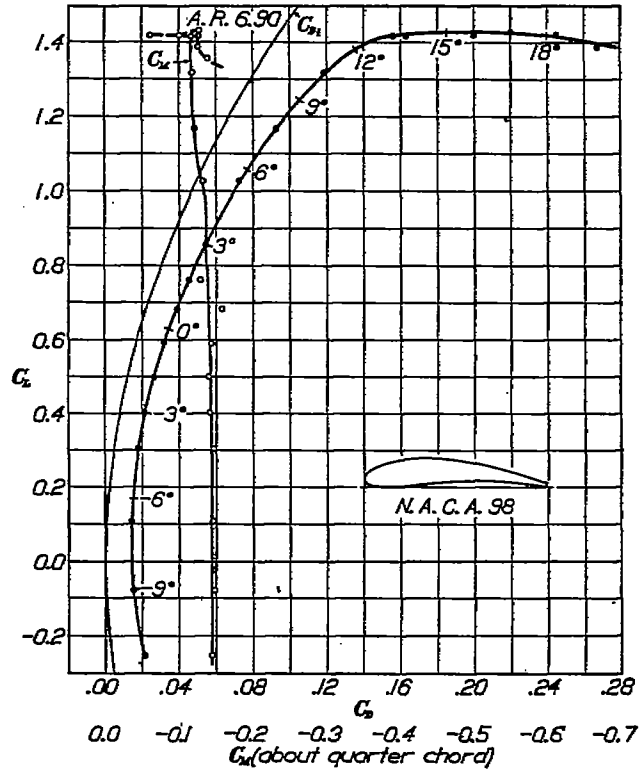


FIG. 20.—Test No. 59-1. Tank pressure 16.2 atmospheres. Dynamic pressure $q=676 \text{ kg/m}^2$. Reynolds Number 2,470,000. Trailing edge milled off square

TABLE V

SECTION NO. N. A. C. A. 97. FICTITIOUS ASPECT RATIO, 6.85.
 MODEL NO. 9. SPAN 30 IN., 76.2 cm TEMPERATURE, 38° C.
 CHORD 5 IN., 12.7 cm PRESSURE, 10.9 ATMOS.
 AREA, 0.0968 m² SPHERES.
 ASPECT RATIO, 6. REYNOLDS NUMBER, 365,000.

Angle of attack, degree	$\frac{q}{kg/m^2}$	Lift L , kg	Lift coef. C_L	Drag coef. C_D
-11.6	700	-14.1	-0.200	0.0354
-9.2	705	-2.05	.030	0.034
-6.7	705	10.75	.158	0.036
-4.1	713	28.42	.354	0.038
-2.8	711	28.82	.419	0.029
-1.6	711	36.65	.533	0.0275
-1.4	710	42.75	.628	0.032
.8	709	45.13	.702	0.036
2.1	704	53.38	.784	0.0472
3.2	704	58.12	.855	0.056
5.6	704	69.04	1.02	0.070
7.9	704	79.03	1.16	0.071
11.1	704	86.48	1.27	0.112
13.4	704	90.23	1.33	0.167
14.3	704	90.64	1.33	0.148
15.4	704	90.07	1.32	0.107
16.4	704	89.55	1.32	0.097
17.0	704	87.48	1.28	0.070

TABLE VI

SECTION NO. N. A. C. A. 97 FICTITIOUS ASPECT RATIO, 6.85.
 (PAINTED).
 MODEL NO. 9. SPAN 30 IN., 76.2 cm TEMPERATURE, 37° C.
 CHORD 5 IN., 12.7 cm PRESSURE, 16.7 ATMOS.
 AREA, 0.0968 m² SPHERES.
 ASPECT RATIO, 6. REYNOLDS NUMBER, 3,060,000.

Angle of attack, degree	$\frac{q}{kg/m^2}$	Lift L , kg	Lift coef. C_L	Drag coef. C_D	Moment about c/4	Moment coef. C_M
-11.9	565	-12.36	-0.226	0.0181	-96.8	-0.189
-9.4	563	-3.26	.059	0.0117	-68.4	-0.098
-7.2	563	6.71	.122	0.0111	-94.5	-0.125
-4.5	563	17.98	.327	0.0186	-100.3	-0.144
-3.2	563	23.63	.406	0.0196	-90.8	-0.130
-1.9	563	28.71	.523	0.0249	-93.6	-0.134
-1.4	563	32.96	.599	0.0300	-92.4	-0.132
.7	563	37.77	.688	0.0367	-97.2	-0.139
1.8	563	41.31	.753	0.0421	-84.1	-0.120
3.0	563	45.97	.822	0.0510	-80.4	-0.124
5.4	563	55.46	1.01	0.0723	-71.3	-0.102
7.6	563	61.33	1.11	0.0834	-69.4	-0.100
10.3	570	70.51	1.29	0.1212	-76.7	-0.099
13.2	565	72.87	1.31	0.1600	-64.5	-0.093
14.4	564	70.23	1.29	0.1783	-17.4	-0.025
15.6	564	66.89	1.28	0.2186	-79.7	-0.115
16.8	564	64.52	1.18	0.2458	-101.2	-0.149

TABLE VII

SECTION NO. N. A. C. A. 98. FICTITIOUS ASPECT RATIO, 6.85.
 MODEL NO. 10. SPAN 30 IN., 76.2 cm AVERAGE TEMPERATURE, 23.5° C.
 CHORD 5 IN., 12.7 cm PRESSURE, 1 ATMOS.
 AREA, 0.0968 m² SPHERE.
 ASPECT RATIO, 6. REYNOLDS NUMBER, 176,000.

Angle of attack, degree	$\frac{q}{kg/m^2}$	Lift L , kg	Lift coef. C_L	Drag coef. C_D
-8.1	27.8	0.01	0.037	0.0632
-6.8	27.8	.38	.141	0.0282
-5.7	27.8	.60	.223	0.0278
-4.4	27.8	.90	.336	0.0290
-2.9	27.8	1.15	.420	0.0314
-1.6	27.8	1.38	.515	0.0347
-.4	27.8	1.66	.621	0.0413
.8	27.8	1.89	.704	0.0463
2.1	28.0	2.14	.792	0.0557
3.2	28.1	2.35	.889	0.0630
4.5	28.1	2.59	.961	0.0708
5.6	28.1	2.80	1.04	0.0799
6.6	28.1	3.03	1.12	0.0920
7.8	27.8	3.20	1.20	0.0995
9.1	27.8	3.35	1.25	0.1078
10.5	27.8	3.58	1.34	0.1238
11.8	27.8	3.68	1.39	0.1306
13.2	27.8	3.72	1.39	0.1356
14.5	27.8	3.75	1.40	0.1710
15.7	27.8	3.74	1.40	0.1895
16.8	27.8	3.71	1.39	0.2083
18.1	27.8	3.69	1.38	0.2268
19.5	27.8	3.65	1.37	0.2502

TABLE VIII

SECTION NO. N. A. C. A. 98. FICTITIOUS ASPECT RATIO, 6.85.
 MODEL NO. 10. SPAN 30 IN., 76.2 cm AVERAGE TEMPERATURE, 27° C.
 CHORD 5 IN., 12.7 cm AREA, 0.0968 m² AT-
 MOSPHERES.
 ASPECT RATIO, 6. REYNOLDS NUMBER, 155,000.

Angle of attack, degree	$\frac{q}{kg/m^2}$	Lift L , kg	Lift coef. C_L	Drag coef. C_D
-9.2	122	-0.96	-0.081	0.0212
-8.1	124	.23	.019	0.0192
-6.8	123	1.49	.123	0.0185
-4.4	125	3.77	.313	0.0225
-2.8	122	4.76	.398	0.0255
-.4	122	6.02	.506	0.0298
.8	122	7.06	.591	0.0333
2.1	124	8.21	.680	0.0410
3.2	124	9.11	.761	0.0464
5.6	125	10.09	.837	0.0545
7.8	125	12.24	1.01	0.0747
10.5	125	13.95	1.15	0.0946
13.2	125	15.29	1.27	0.1188
15.2	125	16.11	1.34	0.1544
16.7	124	16.10	1.33	0.1731
18.8	122	16.09	1.35	0.1933
18.1	122	16.03	1.36	0.2125
19.5	122	16.99	1.35	0.2390
20.7	122	16.79	1.33	0.2619

TABLE IX

SECTION NO. N. A. C. A. 98. FICTITIOUS ASPECT RATIO, 6.85.
 MODEL NO. 10. SPAN 30 IN., 76.2 cm AVERAGE TEMPERATURE, 27° C.
 CHORD 5 IN., 12.7 cm AREA, 0.0968 m² AT-
 MOSPHERES.
 ASPECT RATIO, 6. REYNOLDS NUMBER, 1,400,000

Angle of attack, degree	$\frac{q}{kg/m^2}$	Lift L , kg	Lift coef. C_L	Drag coef. C_D
-9.7	268	-0.16	-0.063	0.0177
-8.8	268	2.91	.117	0.0168
-7.2	259	7.44	.297	0.0200
-4.4	259	12.42	.496	0.0285
-1.6	259	14.63	.586	0.0336
.8	258	16.81	.674	0.0401
2.1	258	18.78	.762	0.0470
5.2	258	20.87	.837	0.0532
7.8	258	24.85	.995	0.0733
10.5	258	28.02	1.12	0.0930
13.2	258	31.33	1.26	0.1170
15.2	258	33.45	1.34	0.1531
16.5	258	33.92	1.37	0.1748
16.7	257	34.36	1.39	0.1938
18.8	256	34.47	1.39	0.2162
19.5	257	34.82	1.40	0.2410
20.7	257	34.64	1.40	0.2688
20.7	257	34.51	1.39	0.2641

TABLE X

SECTION NO. N. A. C. A. 98. FICTITIOUS ASPECT RATIO, 6.85.
 MODEL NO. 10. SPAN 30 IN., 76.2 cm TEMPERATURE, 42.5° C.
 CHORD 5 IN., 12.7 cm PRESSURE, 10.44 ATMOS.
 AREA, 0.0968 m² SPHERES.
 ASPECT RATIO, 6. REYNOLDS NUMBER, 2,880,000.

Angle of attack, degree	$\frac{q}{kg/m^2}$	Lift L , kg	Lift coef. C_L	Drag coef. C_D	Moment about c/4 kg-cm	Moment coef. C_M
-9.2	526	-3.95	-0.078	0.0157	-90.6	-0.140
-8.8	527	5.84	.130	0.0163	-163.0	-0.261
-4.4	527	14.73	.289	0.0182	-87.5	-0.135
-2.8	529	19.44	.380	0.0208	-91.0	-0.140
-1.6	534	26.10	.483	0.0271	-82.3	-0.125
.8	534	29.70	.575	0.0325	-86.5	-0.132
2.1	534	33.92	.656	0.0383	-87.3	-0.133
5.6	531	42.41	.828	0.0455	-84.2	-0.128
7.8	531	51.07	.930	0.0484	-85.2	-0.130
10.5	534	58.12	1.12	0.0507	-73.1	-0.112
13.2	533	65.31	1.27	0.0568	-65.4	-0.100
14.2	533	70.23	1.36	0.0533	7.8	0.012
14.5	532	72.06	1.40	0.0540	-69.6	-0.106
15.7	531	72.20	1.40	0.0445	-73.2	-0.112
16.8	531	72.38	1.41	0.0400	-72.9	-0.112
18.1	531	71.99	1.40	0.0340	-79.5	-0.122
19.5	530	71.27	1.39	0.0271	-79.8	-0.128
20.7	530	70.44	1.37	0.0272	-89.2	-0.137

TABLE XI

SECTION NO. N. A. C. A. 98. FICTITIOUS ASPECT RATIO,
MODEL NO. 10. 6.85.
SPAN 30 IN., 76.2 cm TEMPERATURE, 38° C.
CHORD 5 IN., 12.7 cm PRESSURE, 20.4 ATMOS-
AREA, 0.0968 m² PHERES.
ASPECT RATIO 6. REYNOLDS NUMBER, 3,780,000.

Angle of attack, degree	$\frac{g}{kg}$	Lift $\frac{L}{kg}$	Lift coef. C_L	Drag coef. C_D
-9.2	697	-5.41	-0.080	0.0152
-8.1	698	1.33	.020	.0137
-5.7	698	12.06	.178	.0150
-2.9	697	24.24	.359	.0200
-1.6	697	30.44	.451	.0241
-1.4	698	37.98	.583	.0317
.8	695	43.35	.645	.0374
2.1	695	48.26	.718	.0436
3.2	697	54.19	.802	.0516
5.6	698	65.50	.970	.0701
7.8	698	75.39	1.115	.0895
10.5	703	85.06	1.25	.1148
13.2	703	91.10	1.34	.1610
14.5	704	91.95	1.35	.1725
15.7	696	92.19	1.37	.1914
16.8	696	91.59	1.38	.2100
18.1	701	91.32	1.34	.2365
19.5	699	89.89	1.23	.2668
20.7	697	86.63	1.28	.2824

TABLE XIV

SECTION NO. N. A. C. A. 99. FICTITIOUS ASPECT RATIO,
MODEL NO. 11. 6.85.
SPAN 30 IN., 76.2 cm AVERAGE TEMPERATURE,
CHORD 5 IN., 12.7 cm 27° C.
AREA, 0.0968 m² AVERAGE PRESSURE, 2.03
ASPECT RATIO, 6. ATMOSPHERES.
REYNOLDS NUMBER, 352,000.

Angle of attack, degree	$\frac{g}{kg}$	Lift $\frac{L}{kg}$	Lift coef. C_L	Drag coef. C_D	Moment coef. C_M
-0.4	56.9	-0.16	-0.030	0.0117	0.0285
.7	56.9	.28	.050	.0130	.0001
1.9	56.9	.70	.127	.0187	.0070
3.0	57.5	1.20	.217	.0149	.0042
4.2	57.5	1.64	.295	.0189	.0195
5.5	57.3	2.08	.375	.0221	.0150
6.6	57.3	2.50	.422	.0264	.0015
7.7	57.3	2.95	.583	.0333	.0150
9.4	57.3	3.62	.658	.0439	.0150
11.5	57.3	4.18	.752	.0604	.0260
13.6	57.3	3.86	.895	.1572	.0230
15.2	57.5	3.26	.887	.2000	.0220
16.9	57.2	3.26	.539	.2978	.0500
19.0	57.2	3.26	.589	.2430	.0510

TABLE XII

SECTION NO. N. A. C. A. 98. FICTITIOUS ASPECT RATIO,
(MILLED T. E.). 6.90.
MODEL NO. 10. TEMPERATURE, 39° C.
SPAN 30 IN., 76.2 cm PRESSURE, 16.2 ATMOS-
CHORD 4.95 IN., 12.7 cm PHERES.
AREA, 0.0958 m² REYNOLDS NUMBER, 2,470,000.
ASPECT RATIO, 6.05.

Angle of attack, degree	$\frac{g}{kg}$	Lift $\frac{L}{kg}$	Lift coef. C_L	Drag coef. C_D	Moment about c/4 $\frac{kg \cdot cm}{kg \cdot cm}$	Moment coef. C_M
-11.7	577	-14.39	-0.260	0.0211	-101.0	-0.146
-9.0	577	-4.25	-0.077	.0154	-104.0	-1.139
-6.7	578	6.04	.109	.0142	-102.0	-1.147
-4.4	578	17.10	.308	.0180	-103.0	-1.148
-3.0	578	22.41	.404	.0217	-98.1	-1.143
-1.6	575	27.60	.501	.0265	-97.8	-1.141
-1.4	575	32.74	.594	.0321	-93.8	-1.144
.8	573	37.51	.632	.0396	-110.0	-1.159
1.8	576	42.37	.766	.0455	-90.5	-1.130
3.0	576	47.25	.856	.0543	-95.7	-1.138
5.6	577	56.69	1.03	.0735	-93.5	-1.134
7.7	577	64.90	1.17	.0931	-84.2	-1.121
10.4	579	73.18	1.32	.1192	-83.0	-1.110
13.2	579	78.67	1.42	.1664	-82.1	-1.118
14.4	566	76.98	1.42	.1624	-42.3	-1.062
15.7	579	78.87	1.42	.2004	-72.0	-1.103
16.8	577	79.29	1.43	.2203	-90.6	-1.130
18.1	577	78.29	1.42	.2454	-89.0	-1.128
19.4	577	76.85	1.39	.2876	-88.1	-1.127
20.7	562	72.80	1.36	.2993	-95.2	-1.140

TABLE XV

SECTION NO. N. A. C. A. 99. FICTITIOUS ASPECT RATIO,
MODEL NO. 11. 6.85.
SPAN 30 IN., 76.2 cm AVERAGE TEMPERATURE,
CHORD 5 IN., 12.7 cm 30.5° C.
AREA, 0.0968 m² AVERAGE PRESSURE, 4.06
ASPECT RATIO, 6. ATMOSPHERES.
REYNOLDS NUMBER, 710,000

Angle of attack, degree	$\frac{g}{kg}$	Lift $\frac{L}{kg}$	Lift coef. C_L	Drag coef. C_D
-0.4	120	-0.48	-0.040	0.0134
.7	120	.54	.046	.0132
1.9	120	1.53	.136	.0150
3.0	120	2.46	.211	.0171
4.2	120	3.46	.297	.0194
5.4	120	4.47	.382	.0232
6.6	120	5.38	.460	.0277
7.7	120	6.38	.545	.0334
9.4	120	7.78	.666	.0437
11.5	119	9.32	.805	.0500
13.6	120	9.53	.817	.1125
15.2	119	8.24	.702	.1986
16.8	119	7.64	.651	.2374
19.0	119	7.22	.625	.2645

TABLE XIII

SECTION NO. N. A. C. A. 99. FICTITIOUS ASPECT RATIO,
MODEL NO. 11. 6.85.
SPAN 30 IN., 76.2 cm AVERAGE TEMPERATURE,
CHORD 5 IN., 12.7 cm 26° C.
AREA, 0.0968 m² PRESSURE, 1 ATMOSPHERE.
ASPECT RATIO, 6. REYNOLDS NUMBER, 176,000.

Angle of attack, degree	$\frac{g}{kg}$	Lift $\frac{L}{kg}$	Lift coef. C_L	Drag coef. C_D
-0.4	27.6	-0.08	-0.032	0.0186
.7	27.6	.24	.039	.0173
1.9	27.6	.43	.161	.0186
3.0	27.5	.56	.209	.0207
4.2	27.5	.72	.273	.0266
5.4	27.5	.92	.346	.0290
6.6	27.6	1.14	.427	.0341
7.7	27.6	1.44	.539	.0403
9.4	27.6	1.62	.612	.0536
11.5	27.4	1.92	.722	.0800
13.6	27.4	1.72	.645	.1706
15.2	27.4	1.57	.691	.2034
16.8	27.4	1.50	.566	.2316
19.0	27.4	1.48	.567	.2594

SECTION NO. N. A. C. A. 99. FICTITIOUS ASPECT RATIO,
MODEL NO. 11. 6.85.
SPAN 30 IN., 76.2 cm AVERAGE TEMPERATURE,
CHORD 5 IN., 12.7 cm 31° C.
AREA, 0.0968 m² AVERAGE PRESSURE, 6
ASPECT RATIO, 6. ATMOSPHERES.
REYNOLDS NUMBER, 1,070,-000.

Angle of attack, degree	$\frac{g}{kg}$	Lift $\frac{L}{kg}$	Lift coef. C_L	Drag coef. C_D
-0.4	183	-0.66	-0.037	0.0124
.7	183	.70	.040	.0129
1.9	183	2.22	.126	.0140
3.0	183	3.61	.204	.0156
4.2	183	5.21	.295	.0188
5.4	183	7.04	.396	.0226
6.6	183	8.18	.462	.0270
7.7	183	9.56	.541	.0320
9.4	183	11.92	.672	.0413
11.5	183	14.26	.805	.0553
13.6	183	16.42	.928	.0705
15.2	183	18.28	1.03	.0892
16.8	184	16.14	.906	.1738
19.0	183	16.04	.906	.2057

TABLE XVII

SECTION NO. N. A. C. A. 99. FICTITIOUS ASPECT RATIO, 6.85.
 MODEL NO. 11. SPAN 30 IN., 76.2 cm
 CHORD 5 IN., 12.7 cm
 AREA, 0.0968 m²
 ASPECT RATIO, 6.

AVERAGE TEMPERATURE, 38° C.
 AVERAGE PRESSURE, 8.8 ATMOSPHERES.
 REYNOLDS NUMBER, 1,440,000.

Angle of attack, degree	$\frac{q}{m^2}$	Lift L kg	Lift coef. C_L	Drag coef. C_D
-0.4	257	-1.18	-0.047	0.0120
1.9	256	8.25	.181	.0135
3.0	256	5.20	.209	.0157
4.2	257	7.55	.302	.0169
5.4	258	9.59	.385	.0222
6.6	257	11.80	.473	.0266
7.7	257	13.66	.547	.0320
9.4	255	16.35	.662	.0409
11.5	255	20.34	.822	.0564
13.6	257	23.68	.952	.0723
15.2	258	26.50	1.06	.0839
16.8	257	28.71	1.15	.1078
19.0	256	28.60	1.15	.1595
20.7	256	27.26	1.09	.2310

TABLE XIX

TABLE OF ORDINATES OF AIRFOIL SECTIONS. NOS. 97, 98 AND 99

Station	Airfoil No. 97		Airfoil No. 98		Airfoil No. 99		
	Percent of chord	Upper	Lower	Upper	Lower	Upper	Lower
0	% of chord	4.17	4.17	4.00	4.00	0.00	-0.00
2.5		7.93	.73	8.00	.73	2.50	-2.50
5.0		9.50	.83	9.60	.80	4.33	-4.33
7.5		10.80	.10	10.85	.10	4.90	-4.90
10		11.80	.03	11.93	.00	5.33	-5.33
15		13.30	.00	13.40	.00	6.03	-6.03
20		14.28	.17	14.38	.22	6.43	-6.43
25		14.82	.47	14.96	.56	6.66	-6.66
30		15.15	.83	15.37	1.07	6.99	-6.99
40		15.00	1.73	15.30	2.06	7.36	-7.36
50		13.94	2.50	14.28	2.87	7.63	-7.63
60		13.20	2.86	12.50	3.23	8.03	-8.03
70		9.77	2.80	10.30	3.13	8.50	-8.50
80		6.87	2.80	7.70	2.47	8.83	-8.83
90		3.60	1.93	4.87	1.33	9.23	-9.23
95		1.87	.67	8.27	.56	9.57	-9.57
100		.13	.00	.90	.00	.00	-0.00
Radius of leading edge.		3.57		3.57		3.57	
Radius of trailing edge.				0.93			

TABLE XVIII

SECTION NO. N. A. C. A. 99. FICTITIOUS ASPECT RATIO, 6.86.
 MODEL NO. 11. SPAN 30 IN., 76.2 cm
 CHORD 5 IN., 12.7 cm
 AREA, 0.0968 m²
 ASPECT RATIO, 6.

AVERAGE TEMPERATURE, 40° C.
 AVERAGE PRESSURE, 16.24 ATMOSPHERES.
 REYNOLDS NUMBER, 2,950,000.

Angle of attack, degree	$\frac{q}{m^2}$	Lift L kg	Lift coef. C_L	Drag coef. C_D	Moment coef. C_M
-0.4	544	-2.21	-0.043	0.0109	0.0028
.7	544	2.16	.041	.0106	-.0034
1.9	544	6.77	.129	.0117	.0012
3.0	544	11.51	.218	.0138	.0029
4.2	547	16.34	.309	.0165	.0038
5.4	545	20.49	.389	.0201	.0100
6.6	544	24.82	.471	.0246	.0080
7.7	538	28.83	.555	.0292	.0100
9.4	543	35.63	.678	.0390	.0180
11.5	543	43.19	.823	.0562	.0010
13.6	540	49.81	.950	.0702	.0990
15.2	540	55.82	1.06	.0845	.0890
16.8	541	53.89	1.02	.148	-.0290
19.0	540	45.55	.928	.225	-.0780
20.7	537	45.08	.888	.280	-.1150

REFERENCES

- Max M. Munk: The Modification of Wind Tunnel Results by the Wind Tunnel Dimensions. Journal of Franklin Institute, August, 1923.
- Max M. Munk: Elements of the Wing Section Theory and of the Wing Theory. N. A. C. A. Technical Report No. 191. 1924.
- Max M. Munk: The Determination of the Angles of Attack of Zero Lift and Zero Moment, Based on Munk's Integrals. N. A. C. A. Technical Note No. 122. 1923.

APPENDIX
COMPARISON WITH THEORY

By George J. Higgins

In this appendix, the aerodynamic properties of the N. A. C. A. airfoil No. 97 are computed as far as the present theory allows. This comprises the computation of the lift and the moment characteristics at any angle of attack.

The lift characteristics.—The angle of attack, at which the lift force is zero, is first computed. The method employed is obtained from the N. A. C. A. Technical Note No. 122 (Reference 3). The five-point method is used because of its greater accuracy.

$$-\alpha_{L_0} = F_1 \frac{\xi_1}{c} + F_2 \frac{\xi_2}{c} + \dots + F_n \frac{\xi_n}{c} + \dots$$

in degrees where,

α_{L_0} = angle of attack at which the lift is zero.

ξ = ordinate of the mean camber line at a point (x) on the chord line, minus the ordinate of the trailing edge.

c = the chord of the airfoil.

$$\alpha_{L_0} = \sum \xi f = f_1 \xi_1 + f_2 \xi_2 + f_3 \xi_3 + f_4 \xi_4 + f_5 \xi_5 \quad (\text{Reference 3})$$

$$x_1 = 99.458\%c$$

$$f_1 = 1252.24$$

$$\xi_1 = 0.13\%c$$

$$x_2 = 87.426\%c$$

$$f_2 = 109.048$$

$$\xi_2 = 2.91\%c$$

$$x_3 = 50.000\%c$$

$$f_3 = 32.596$$

$$\xi_3 = 8.16\%c$$

$$x_4 = 12.574\%c$$

$$f_4 = 15.684$$

$$\xi_4 = 6.31\%c$$

$$x_5 = 0.542\%c$$

$$f_5 = 5.978$$

$$\xi_5 = 3.71\%c$$

$$-\alpha_{L_0} = \sum f \xi = 1.63 + 3.17 + 2.66 + 0.989 + 0.222$$

$$\alpha_{L_0} = -8.671^\circ \sim 8^\circ 40'$$

This value agrees well with the observed value. A graphical determination is also made by the two methods shown in the accompanying diagram (Fig. 21).

The angles determined there are:

One-point method,
 $\alpha_{L_0} = -9^\circ 15'$

Two-point method,
 $\alpha_{L_0} = -8^\circ 50'$

The lift force and the lift coefficient for any other angle of attack are obtained from the following expressions (Reference 2):

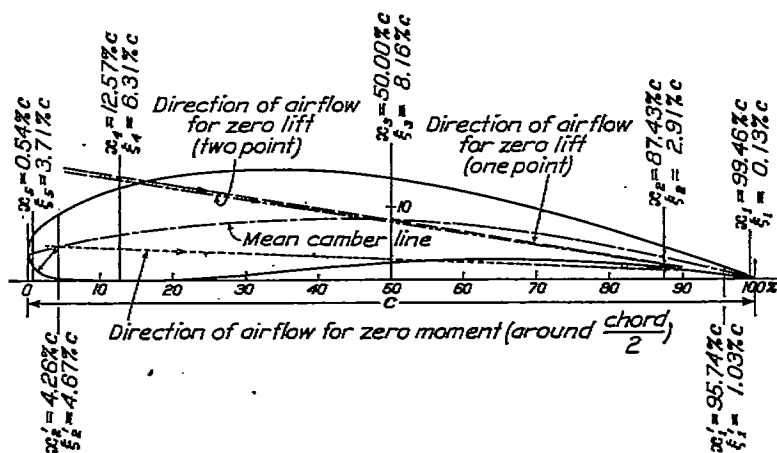


FIG. 21.—Angles of zero lift and zero moment (around $\frac{\text{chord}}{2}$). Airfoil N. A. C. A. No. 97.
Found by computation

$$L = 2\pi\alpha \text{ (radians)} \frac{\rho}{2} V^2 S \frac{1}{1 + \frac{b^2}{b^2}}$$

$$= \frac{2\pi\alpha \text{ (degrees)} qS}{57.3 \left[1 + \frac{2S}{b^2} \right]}$$

$$C_L = \frac{L}{qS} = \frac{2\pi\alpha \text{ (degrees)}}{57.3 \left[1 + \frac{2S}{b^2} \right]}$$

where

- L = lift force
- α = angle of attack
- ρ = density
- V = velocity
- S = surface area
- b = span
- q = dynamic pressure

For the N. A. C. A. No. 97 airfoil,

$$\begin{aligned} S &= 0.0968 \text{ m}^2 \\ b &= 0.762 \text{ m} \end{aligned}$$

$$\begin{aligned} C_L &= \frac{2\pi\alpha \text{ (degrees)}}{57.3 \left[1 + \frac{2 \times 0.0968}{(0.762)^2} \right]} \\ &= .0822 \alpha \text{ (degrees)} \\ \frac{dC_L}{d\alpha \text{ (degrees)}} &= .0822 \end{aligned}$$

The slope of the observed lift coefficient curve has a magnitude that is about 86 per cent of that computed.

$$\frac{dC_L}{d\alpha} \text{ (observed)} = .0710$$

The moment characteristics.—The angle of attack, at which the moment about the 50 per cent point of the chord is zero, is computed first in determining the moment. The method is also obtained from the N. A. C. A. Technical Note No. 122 (Reference 3).

$$\alpha_{M_0} = 62.634 \left[\frac{\xi_1}{c} - \frac{\xi_2}{c} \right]$$

where,

α_{M_0} = angle of attack, at which the moment about the 50 per cent point of the chord is zero.

ξ = ordinate of the mean camber line at a point (x) on the chord, minus the ordinate of the trailing edge.

$$\begin{aligned} x_1 &= 95.74\% c. & \xi_1 &= 1.03\% c. \\ x_2 &= 4.26\% c. & \xi_2 &= 4.67\% c. \\ \alpha_{M_0} &= 62.634 (1.03 - 4.67) \\ &= -2.28^\circ \sim -2^\circ 17' \end{aligned}$$

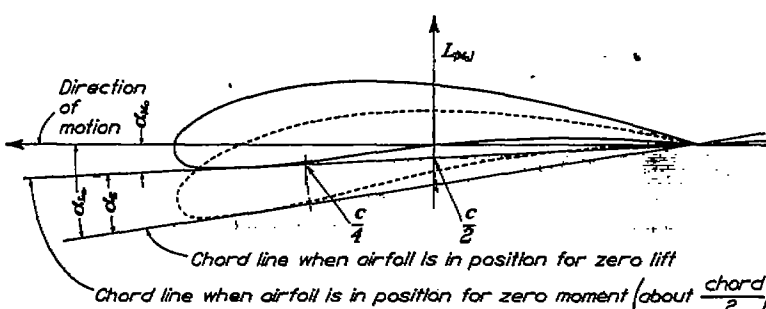


FIG.-22

The graphical construction shown in the diagram (Fig. 21), gives:

$$\alpha_{M_0} = -2^\circ 20'$$

The effective angle, corresponding to the lift at the angle for zero moment, is next determined from the values of the angles for zero lift and zero moment (Fig. 22).

$$\alpha_{L_0} = \text{angle of attack for zero lift} = 8^\circ 40'$$

$$\alpha_{M_0} = \text{angle of attack for zero moment} = 2^\circ 17'$$

$$\alpha_s = \text{effective angle.}$$

$$\begin{aligned} \alpha_s &= \alpha_{L_0} - \alpha_{M_0} \\ &= 8^\circ 40' - 2^\circ 17' \\ &= 6^\circ 13' \sim 6.216^\circ \end{aligned}$$

When the airfoil is in the position such that the moment about the 50 per cent point of the chord is zero, the resultant force passes through this point. Neglecting the moment due to the drag force, which is very small, the moment about any other point on the chord can be computed by obtaining the product of the lift force and its lever arm about that point. By this method, the magnitude of the moment about a point at 25 per cent of the chord is determined. This moment is theoretically constant for all angles of attack and values of lift. When plotted against the lift, the curve will be a straight line parallel to the lift axis.

$$M = L \times l = \frac{2\pi\alpha_E q S}{57.3} \times \frac{l}{l + \frac{b^2}{4}}$$

where:

M = moment about 25 per cent of chord

L = lift

l = lever arm = $-\frac{c}{4}$

c = chord = 12.7 cm

α_E = effective angle of attack = 6.216°

q = dynamic pressure = 530 kg/m²

S = surface area = .0968 m²

b = span = .762 m

$$M = \frac{2\pi \times 6.216 \times 530 \times .0968 \times (-12.7) \times .994}{57.3 \left[1 + \frac{2 \times .0968}{(.762)^2} \right] \times 4} = -83.0 \text{ kg cm}$$

$$C_x = \frac{M}{qSc} = \frac{-83.0}{530 \times .0968 \times 12.7} = -0.1275$$

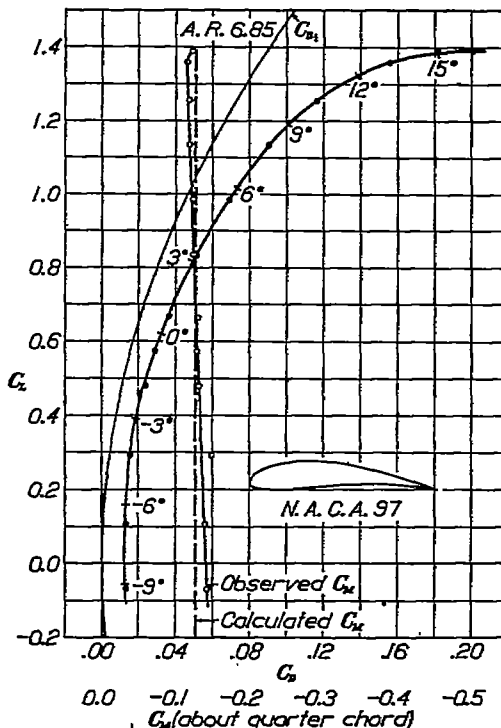


FIG. 23.—Test 60-7. Tank pressure 15.9 atmospheres. Dynamic pressure $q=530 \text{ kg/m}^2$. Reynolds Number 2,920,000. Airfoil with two skids

The computed and the observed values of moment coefficient are shown in the chart of observed values for the N. A. C. A. No. 97 airfoil, Figure 23, for purposes of comparison.